

Elsevier Editorial System(tm) for Marine and
Petroleum Geology
Manuscript Draft

Manuscript Number: JMPG-D-18-01217

Title: An Integrated Approach to Fracture Characterization of the Kraka Field

Article Type: Full Length Article

Keywords: reservoir characterization; structural correlation; borehole images; core analysis; seismic attribute volumes; ant-tracking; chalk; Danish North Sea.

Corresponding Author: Miss Tala Maria Aabø, MSc

Corresponding Author's Institution: University of Copenhagen

First Author: Tala Maria Aabø, MSc

Order of Authors: Tala Maria Aabø, MSc; Jesper Sören Dramsch, MSc; Camilla Louise Wurtzen, MSc; Solomon Seyum, Ph.D.; Frédéric Amour, Ph.D.; Michael Welch, Ph.D.

Abstract: Oil and gas production of tight chalk reservoirs frequently rely on the presence of natural fractures, which increases the effective permeability of the reservoirs. Knowledge of these fracture systems can therefore be used strategically in well planning as well as in IOR and EOR efforts. Here we present an integrated workflow for fracture characterization in chalk, developed in the Kraka Field, located in the Danish sector of the North Sea. The workflow is based on data from borehole images, cores and seismic. By introducing two ant-tracked attribute volumes, which display structural trends below the resolution of amplitude seismic, we are able to correlate features at different scales. In Kraka, this approach has revealed that the fracture pattern is more complex than previously suggested. We propose that fracture generation and propagation in the field is in part controlled by the regional maximum horizontal stress and in part formed in response to salt movements.

Suggested Reviewers: Peter Frykman Ph.D.
Senior Research Geologist, GEUS
pfr@geus.dk

Lars Ole Boldreel Ph.D.
Associate Professor, Department of Geography and Geology, Copenhagen University
lob@ign.ku.dk

Stein Inge Pedersen
Schlumberger Stavanger Research
stein.inge.pedersen@slb.com

Romain Prioul Ph.D.
Schlumberger-Doll Research
rprioul@slb.com

Research Data Related to this Submission

There are no linked research data sets for this submission. The following reason is given:

Data will be made available on request

September 25th, 2018

Editorial department of Journal of Marine and Petroleum Geology

Istituto Nazionale di Oceanografia e di Geofisica Sperimentale

Sgonico, Italy

Dear Dr. Massimo Zecchin,

We are happy to submit our manuscript entitled “An Integrated Approach to Fracture Characterization of the Kraka Field” for consideration of publication in Journal of Marine and Petroleum Geology. The manuscript has not been published elsewhere nor has it been submitted simultaneously for consideration elsewhere.

We present a new workflow for subsurface fracture characterization, based on cores borehole images and seismic. The scale-gap between well data and conventional (amplitude) seismic is reduced by the introduction of two ant-tracked seismic cubes. These cubes enhance subtle features below the resolution of conventional seismic, allowing for correlation of structural features at different scales. The information and understanding of natural fracture systems obtained through this workflow can be used strategically in the E&P industry (e.g. for EOR and IOR purposes), and we believe it is in good correspondence with the scope of your journal.

On behalf of the co-authors,

Tala Maria Aabø

Ph.D. fellow,

Natural History Museum of Denmark

*Highlights (for review)

Highlights: An Integrated Approach to Fracture Characterization of the Kraka Field

- Combined analyses of borehole images (BHIs) and core sections provide reliable fracture interpretations for usage in e.g. reservoir characterization.
- Ant-tracked seismic volumes, preferably generated through RGB-processing, reduces the scale-gap between well data (BHIs and cores) and conventional amplitude seismic. Thus allowing for extrapolation of fractures away from boreholes and calibration of 3D models, such as fracture network models.
- The presented integrated workflow provides insight into the upscaling process.
- In Kraka, the approach has revealed a more complex fracture pattern than previously assumed.

An Integrated Approach to Fracture Characterization of the Kraka Field

T.M. Aabø, J.S. Dramsch, C. L. Würtzen, S. Seyum, F. Amour and M.J. Welch

September 25, 2018

1 Abstract

Oil and gas production of tight chalk reservoirs frequently rely on the presence of natural fractures, which increases the effective permeability of the reservoirs. Knowledge of these fracture systems can therefore be used strategically in well planning as well as in IOR and EOR efforts. Here we present an integrated workflow for fracture characterization in chalk, developed in the Kraka Field, located in the Danish sector of the North Sea. The workflow is based on data from borehole images, cores and seismic. By introducing two ant-tracked attribute volumes, which display structural trends below the resolution of amplitude seismic, we are able to correlate features at different scales. In Kraka, this approach has revealed that the fracture pattern is more complex than previously suggested. We propose that fracture generation and propagation in the field is in part controlled by the regional maximum horizontal stress and in part formed in response to salt movements.

Keywords: reservoir characterization, structural correlation, borehole images, BHIs, resistivity images, FMS, FMI, core analysis, seismic attribute volumes, ant-tracking, chalk, Danish North Sea.

2 Introduction

Chalks typically represent high porosity - low permeability reservoirs, in which natural fractures are essential for hydrocarbon production (*Koestler & Reksten, 1992*). Fracture characterization is therefore imperative in optimizing production schemes and obtaining economically viable recovery factors. Accurate predictions of natural fracture systems require an understanding of the controls on fracture orientations and distributions in an area (*Fernø, 2012*). We have developed a workflow to correlate structural features at different scales, based on borehole image, core and seismic data. The applied seismic data includes an amplitude volume and two ant-tracked volumes. High resolution lineations mapped on the two ant-tracked cubes (generated through a variance cube and through RGB-image processing of the 3D seismic volume, respectively) enables detection of smaller-scale lineations below the resolution of conventional seismic, thus bridging the scaling-gap between well and seismic data.

The Kraka Field, an asymmetric anticlinal structure located in the Danish Central Graben (Figure 1), was chosen as a test-case as it is a relatively simple structure with a manageable amount of data. Kraka is produced mainly from the Danian Ekofisk Formation but also from the Maastrichtian Tor Formation, both of which are naturally fractured chalk reservoirs (*Jørgensen & Andersen, 1991*). Combining the three data types in an integrated workflow allows for the extrapolation of fractures away from the borehole, increasing our holistic understanding of the natural fracture distribution in the Kraka Field. Results from this study will serve as inputs into a discrete fracture network model (DFN) founded on geomechanical principles for fracture propagation, which will improve future well planning and EOR activities in the area. Using this integrated approach we are able to evaluate orientations of lineations from well- to seismic scale, allowing for structural modelling based on a geological conceptual model.

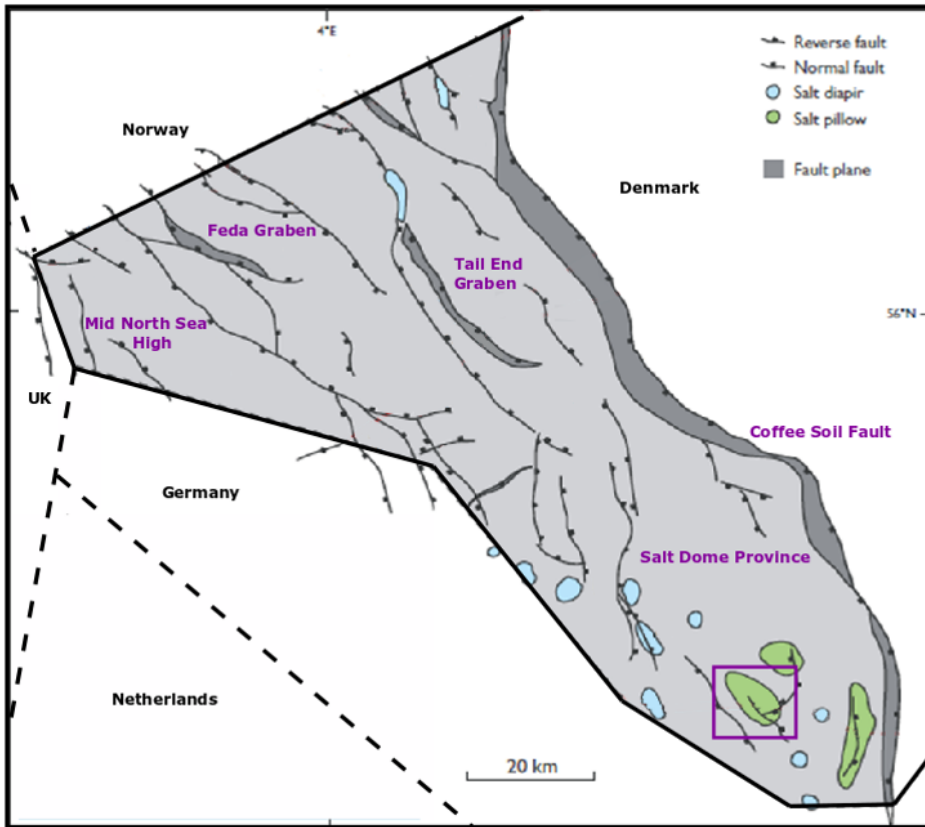


Figure 1: Location of the Kraka Field, indicated by the purple square, on a structural elements map of the Danish Central Graben (after Møller & Rasmussen, 2003).

The Kraka anticline was induced through halokinesis. Initiation started during the Triassic and continued to move during the remaining Mesozoic (Rank-Friend & Elders, 2004). The structure stretches more than 8km along its long axis and approximately 5km along its short axis (Rasmussen *et al.*, 2005). The lithology in Kraka varies between pure chalk and marly chalk, with varying amounts of chert layers and nodules. Cores from the field show localized staining which is cyclic and often associated with the chert. On well-scale, three main structural features have been identified in Kraka. Large, open fractures with slickensides are abundantly observed throughout the core data. These fractures commonly terminate in clay rich layers. Smaller, chert-associated fractures occur frequently within the Ekofisk Formation and on occasion within the Tor Formation. Styolite-associated fractures, which is predominantly observed in the Tor formation, are perpendicular to the pressure solution seems and are typically <25mm high.

Both reservoir units are characterized as tight. Porosities are in the range of 20-35% and permeabilities range from 3mD to <1 mD (Klinkby *et al.*, 2005). Matrix permeabilities in the field are significantly enhanced due to the presence of these natural fractures. The tectonic fractures (shear and extensional) are the main permeability enhancers. Smaller fractures associated with cherts and stylolites may however be important for local permeability enhancement (Jørgensen *et al.*, 1991).

It has previously been concluded that tectonic fracturing in the Kraka chalk may be understood as simple dome related fractures, possibly dominated by a tangential system. It was also suggested that Kraka fractures occur in swarms: a production logging tool from a horizontal wellbore indicated that only 4 of the 17 perforation intervals in that well contributed 94 % of the fluid production (Jørgensen & Andersen, 1991). The potential existence of fracture swarms is further addressed in this study. Moreover, we propose that the Kraka fracture pattern is more complex than previously suggested with a primary set of fractures controlled by the regional maximum horizontal stress as well as a secondary set of dome-related fractures, associated

with halokinesis.

3 Workflow: Data Availability, Consistency and Correlation

In this study, the natural fracture pattern of the Kraka Field was interactively characterized through bore-hole images (BHIs) and cores, prior to structural correlation with seismic data. The fracture characterization effort was primarily focused on the lateral fracture distribution, as the majority of Kraka wells are horizontal. Main emphasis has been put on the Ekofisk section, as it constitutes the primary target of these wellbores. Seismic was used to map faults and fracture zones away from the borehole and to identify regional structural trends.

The full integrated approach is schematically shown in Figure 2. Specific details of each step are given in the following subsections.

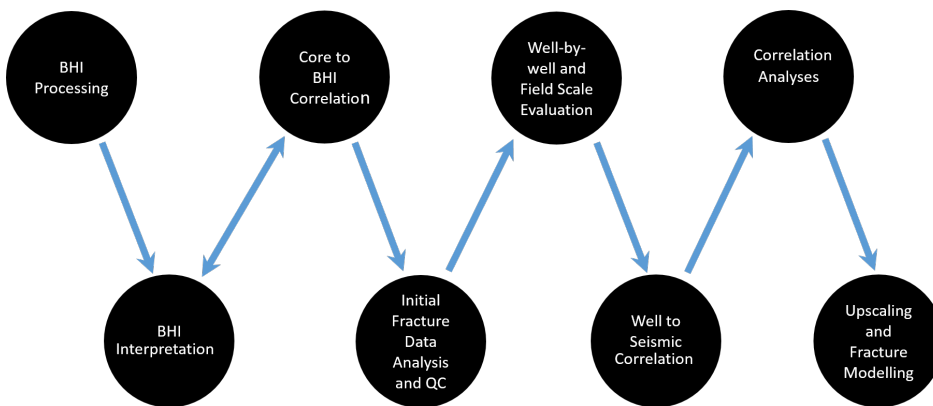


Figure 2: Integrated workflow.

3.1 Processing and Treatment of Borhole Images

Borehole image data was acquisitioned in 10 Kraka wells drilled in the time period between 1989 and 1997. Microresistivity data was obtained in seven well sections, using either the Formation MicroScanner (FMS) tool or the Formation MicroImager (FMI) tool. The remaining three wells, which were surveyed using measurement while drilling technology, have been excluded from this study due to poor data resolution. In the first step of the workflow, the microresistivity data were manually processed in Techlog, following the Schlumberger standard outline, illustrated in Figure 3.



Figure 3: Processing of BHI Data.

Of the wells surveyed by FMS and FMI tools, one is vertical, one is deviated at approximately 70° at reservoir level and five are horizontal (Table 1).

Well	Orientation	Tool	Length (m)
Well 1	Horizontal	FMS	691
Well 2	Deviated	FMS	730
Well 3	Horizontal	FMS	1987
Well 4	Horizontal	FMI	1704
Well 5	Horizontal	FMI	2391
Well 6	Horizontal	FMI	1681
Well 7	Vertical	FMI	205

Table 1: Summary of Studied BHI Sections

Compared to newer image data, Kraka BHIs are of relatively poor image quality and internal image quality variations typically occur within single well sections. This is largely due to tool sticking, artificial signals and key seating, which is observed in most borehole images from the Kraka Field. Chalk sections directly below chert bands have been particularly hard to resolve, as the chert bands do not have planar surfaces and so cause errors in the pad alignment stage of processing. The cherts, being highly resistive compared to the chalk, are in turn well resolved. Consequently, so are chert associated fractures.

Moreover, the reservoir chalk is characterized by internal non-planar resistivity contrasts (that are not an expression of bedding features), which may confuse automatic dip-picking algorithms and lead to incorrect picks. All images have therefore been manually interpreted according to dip-picking principles for horizontal wellbores.

Dip picks were subsequently subjected to structural dip removal (with respect to top reservoir) and fracture densities were subjected to Terzaghi correction. The latter corrects for the sampling bias due to the orientation of the horizontal Kraka well pattern, which was drilled in a predominant NW-SE direction (Figure 4), allowing us to compute true densities of different fracture sets. This is essential to distinguish geological controls on fracture orientation from the effects of borehole orientation.

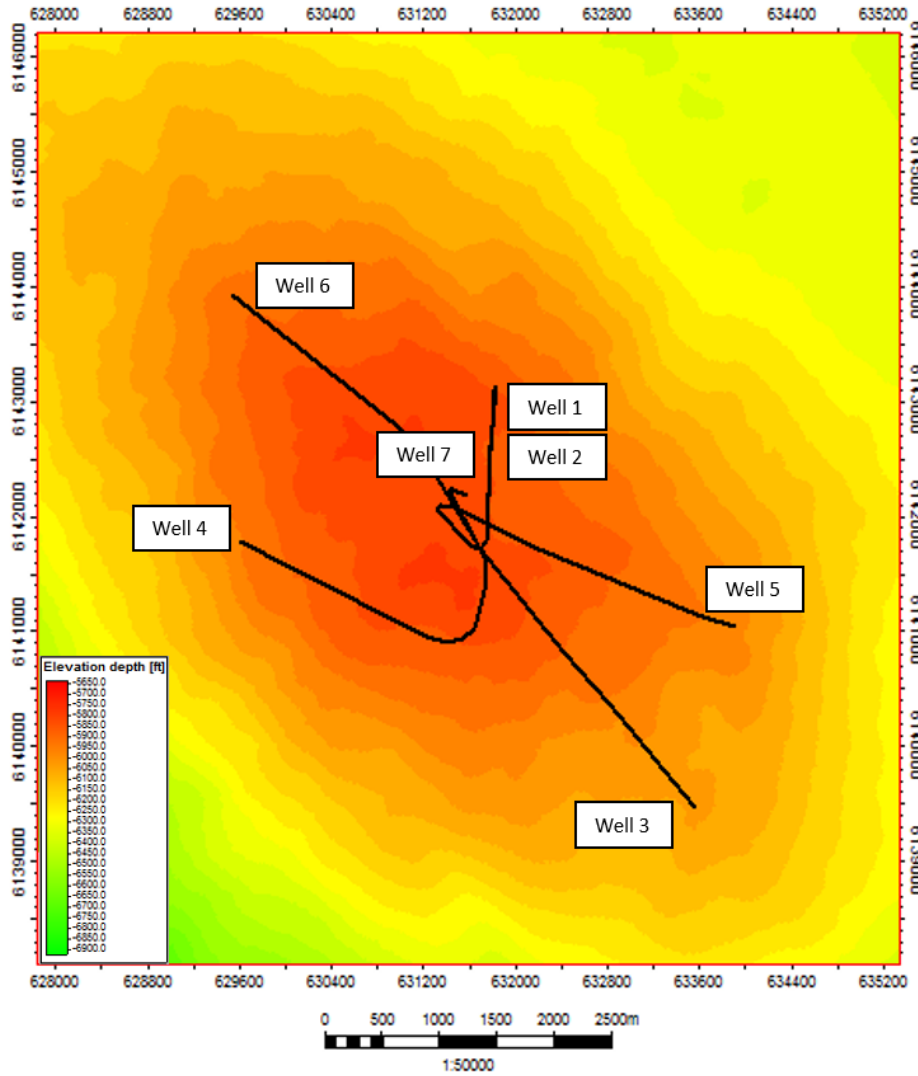


Figure 4: Well pattern of Kraka wells included in this study.

3.2 BHI to Core correlation

The image interpretation scheme was developed through interactive evaluation of core data in the second and third step of the workflow. Cores were available for three of the BHI-surveyed well sections (wells 1,2 and 7). Depth matching between borehole images and cores was enabled by chert occurrences. Since the cherts are highly resistive compared to the reservoir chalk, they are easily identifiable on BHIs across the field. In the absence of a chert layer or nodule, core-to-log calibration is based on fractures.

Depth shifts along wells vary by up to 8 ft. Relative fracture orientations measured in core have been reoriented, depth shifted and plotted alongside image fracture-picks in the applied software.

Correlation between borehole images and cores is considered highly beneficial because:

1. BHI and core data are complementary. Borehole images provide true orientations and survey the reservoir in-situ, so we can differentiate open and closed fractures under reservoir conditions. The advantage of core is that we can identify smaller-scale stylolite associated fractures that are not detectable on

images because the image resolution is about 1-2mm.

- 2
 - 3
 - 4
 - 5
 - 6
 - 7
 - 8
 - 9
 - 10
 - 11
 - 12
 - 13
 - 14
 - 15
 - 16
 - 17
 - 18
 - 19
 - 20
 - 21
 - 22
 - 23
 - 24
 - 25
 - 26
 - 27
 - 28
 - 29
 - 30
 - 31
 - 32
 - 33
 - 34
 - 35
 - 36
 - 37
 - 38
 - 39
 - 40
 - 41
 - 42
 - 43
 - 44
 - 45
 - 46
 - 47
 - 48
 - 49
 - 50
 - 51
 - 52
 - 53
 - 54
 - 55
 - 56
 - 57
 - 58
 - 59
 - 60
 - 61
 - 62
 - 63
 - 64
 - 65
2. In the BHI data from the Kraka Field, sinusoids representing bedding (chalk and marl) are continuous across borehole images. Most fractures are however only represented by partial sinusoids, either because they are short or because they are only partially open or cemented. Comparison with core data, when available, is imperative in determining which partial signals should be picked. Lessons learned from cored wells are transferable to BHI-surveyed wells without core.
3. In terms of azimuth, the dip-picking tools in the applied software (as in most commercial packages) are highly sensitive to small “tweaks”. This means that the orientation given by tadpoles can change drastically depending on how the partial fracture signal is picked. Where there is ambiguity, we have picked partial sinusoids to be consistent with nearby full sinusoids on borehole images, and calibrated against the fractures in core, where possible.

There is a general good correspondence between orientations of fractures identified in core and fractures picked on borehole images. An example from vertical well 7 is given in Figure 5, which shows a logged core interval (a) with corresponding BHI section (b).

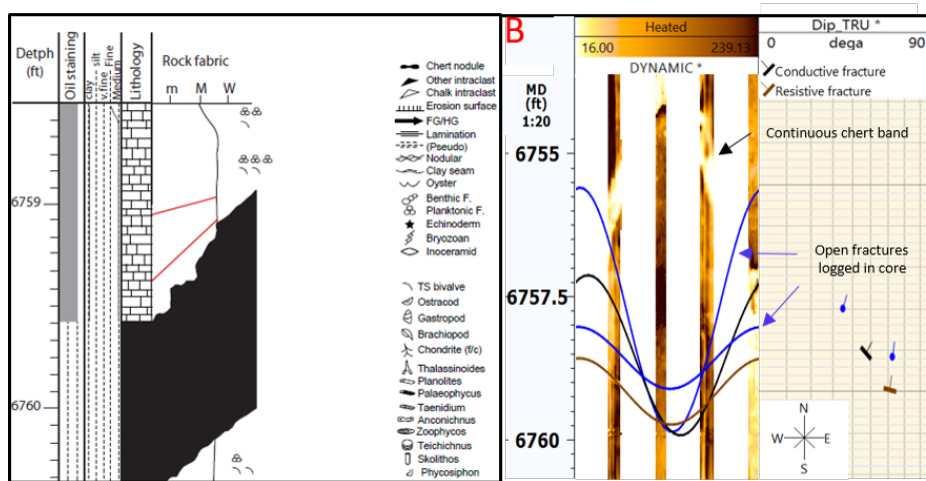


Figure 5: Core log (a) with faults in red and Core-to-BHI correlation (b) of fractured interval in the vertical wellbore.

The core contains two natural fractures, represented by blue tadpoles in the borehole image. These are recognised as natural fractures in core by the presence of slickensides. In the core section, both fractures are open. However, the logged fractures coincide with one open (conductive) and one closed (resistive) fracture picked on the image section. In this case, the image interpretation is considered reliable as BHIs represent the in-situ reservoir conditions. The closed fracture observed on borehole images could possibly have been opened during the coring process itself.

The dip and azimuth of both fractures identified in BHI match the orientation of the fractures logged in core within 12°. In general, dip angles of core- and BHI fracture picks fit to within 9° or less, while dip azimuths are associated with a higher degree of uncertainty. Small discrepancies are to be expected, as core must be reoriented manually to calculate true orientations. Therefore fracture orientations from BHIs are considered the most reliable, while the presence and type of fractures can be identified in the core.

Core-fracture densities are 44% and 36% higher than BHI-fracture densities in wells 1 and 2, respectively (Figure 6). Stylolite occurrences in the chalk accounts for some of the disparity, as they are not resolved in the images. Moreover, fractures located in bioturbated zones and well-parallel fractures are difficult to distinguish in the BHIs. The remaining discrepancy is linked to the quality and resolution of images. The fracture density percentage for well 7 has not been computed, as there are few data points to compare,

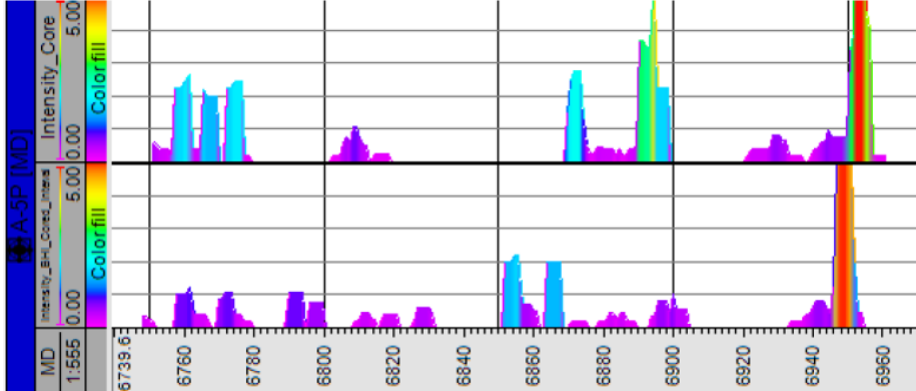


Figure 6: Corrected fracture intensity logs of core-fractures (top) and BHI-fractures in the cored interval (bottom) in well 2. Fracture densities range from 0 in purple to 5 in red.

Stereonets, rose diagrams and fracture intensity logs for wells 1-7 were developed in Petrel during the initial fracture data analysis and quality control step of the workflow (step 4). These were evaluated well-by-well and on field scale during step 5. Here, cumulative fracture densities and spacings were also statistically evaluated to determine the regime of fracture spacing and to evaluate the existence of possible fracture swarms in Kraka.

Cumulative fracture spacings should follow a straight line through a log-log plot in the case of a Power law distribution or in a log-linear plot in the case of a random distribution. A power law regime implies clustering of fractures and may indicate fracture swarms (*Gillespie et al. 1993, 2001*). These often form when propagating fractures causes the stresses ahead of the tip to be more tensile, promoting the growth of nearby fractures, in a similar manner to the process zone often observed around igneous dykes (*Olson, 2003*). The degree of clustering in the fracture point data, and therefore tendency for swarm occurrence, is defined by the following ratio:

$$R = \frac{\text{standard deviation of cumulative fracture spacings}}{\text{mean of cumulative fracture spacings}} \quad (1)$$

A ratio >1 implies fracture clustering and the presence of swarms. A ratio of 1 implies a random fracture distribution, which may form at lower stresses and with lower stress intensity at the fracture tips (*Olson, 2004*).

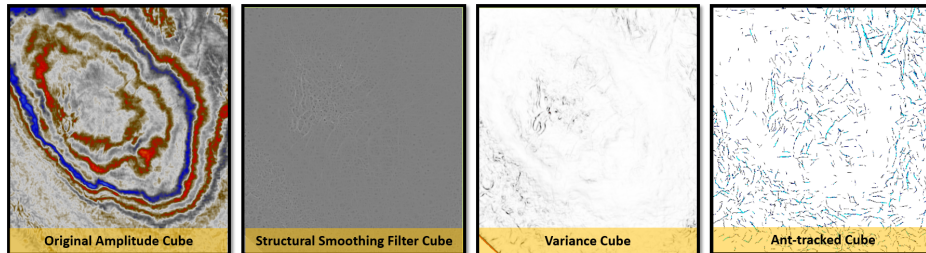
3.3 BHI to Seismic Correlation

Fracture picks from BHIs and cores were subsequently compared to a structural framework derived from the amplitude seismic volume, provided by Maersk, as well as to two ant-tracked structural models in step 6 of the workflow. The seismic amplitude cube (in depth), acquired in 2012, has a vertical resolution in the order of 40 m (sampling rate of 4ms). The ant-tracked volumes enhance subtle faults and fracture zones that are below this vertical resolution. The ant-tracking algorithm systematically analyzes a seismic input cube – mimicking the swarm intelligence of ants (*Pedersen et al., 2005*). Here, a large number of agents (ants) are distributed in the volume. Each ant propagating through the cube is programmed to detect continuous structural lineations. Confidence levels are assigned depending on the length and width of the path of segments.

The first ant-tracked volume was generated in Petrel according to the following workflow (Figure 7):

1. Cropped the original amplitude cube to speed up calculation.

- 1 2. Generated a structural smoothing/median filter cube to increase horizontal continuity and to pick
 2 out the more consistent structural features. The optimal degree of smoothing was achieved through
 3 adjusting the attribute parameter and observing its effect on the smoothing cube (in real time) prior
 4 to realization.
- 5 3. Extracted the variance/chaos cube from the smoothing cube to highlight discontinuities. The variance
 6 cube software is based on wavelet analysis. It calculates the direct measurement of dissimilarity rather
 7 than the inferred similarity of seismic data, producing sharper, more distinct results than those with
 8 traditional coherency techniques (*Schlumberger, 2006*).
- 9 4. Ran ant-tracking algorithm to enhance discontinuities.



23 Figure 7: Workflow for generating ant-tracked volume from the seismic depth cube of the Kraka Field in
 24 Petrel.

25 The second ant-tracked volume was generated in eXchroma and Petrel according to the following work-
 26 flow:

- 27 1. Cropped the original amplitude cube to speed up calculation.
 28 2. Applied the structurally sharpened red-green-blue method, which uses the simultaneous rendering of
 29 multiple depth slices in continuous RGB color to highlight geophysical heterogeneities representative
 30 of geologic features, to the amplitude cube (*Laake, 2015*). The result is an image processed photo-style
 31 cube.
 32 3. Ran ant-tracking algorithm to enhance discontinuities.

33 The vertical resolution of the wavelet based ant-tracked volume is 24ms (7 times the sampling rate). In
 34 the RGB ant-tracked cube, the vertical resolution is 12ms (3 times the sampling rate). The latter cube has
 35 therefore been preferentially used in this study (Figure 8).

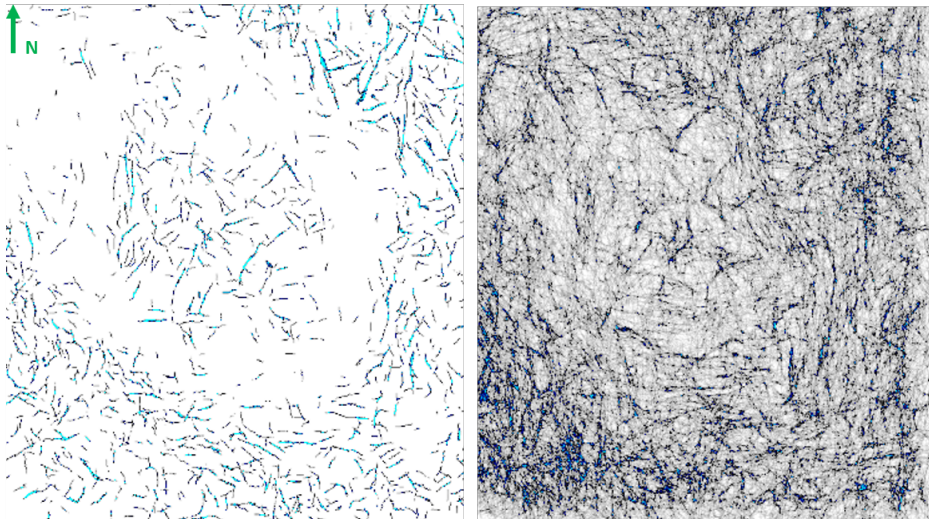


Figure 8: Comparison of the wavelet-based (left) and the RGB-based (right) ant-tracked volumes.

To guide the seismic interpretation and to avoid misclassification of noise or acquisition artifacts, the additional structural information was used as an opaque overlay on the conventional amplitude cube (Figure 9). Dip and azimuth values have been averaged along the fault planes of each interpreted fault to allow for direct comparison with well-scale data in stereonet projections in the seventh and final step of the workflow.

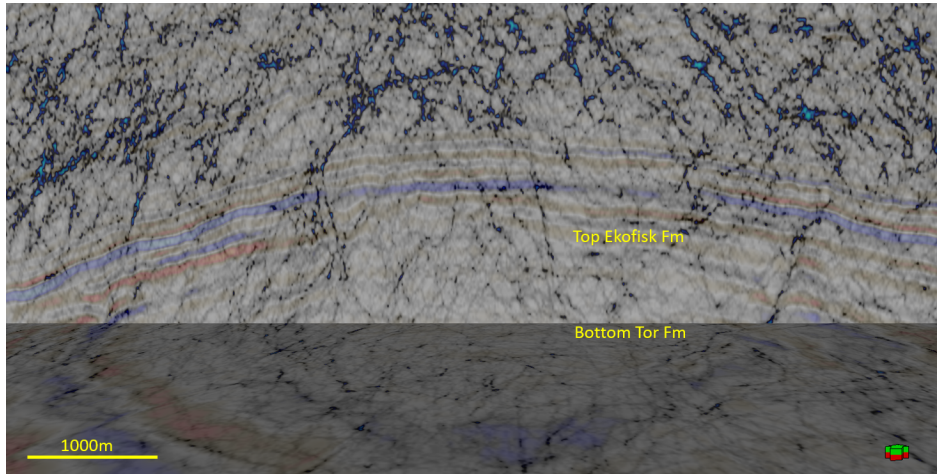


Figure 9: Amplitude-cube over the Kraka Field with the RGB volume as opaque overlay, used for seismic interpretation

4 Well-scale Fracture Trends

4.1 Fracture Densities and Fracture Swarms

Figure 10 shows the fracture orientations in the four NW-SE oriented horizontal wells prior to- and after applying the Terzaghi correction for borehole orientation. According to expectations, the uncorrected strike rose diagrams are dominated by NE-SW striking fractures, as the fracture density depends on the angle between the well trajectory and the fracture planes. After correction however, the rose diagrams largely remain unchanged, indicating that the fracture orientation is real, and not just an apparent effect due to

well orientation. Note however that in 2 wells (wells 3 and 4) the Terzaghi correction also reveals another fracture set, near parallel to the wellbore, that cannot be identified on the uncorrected data.

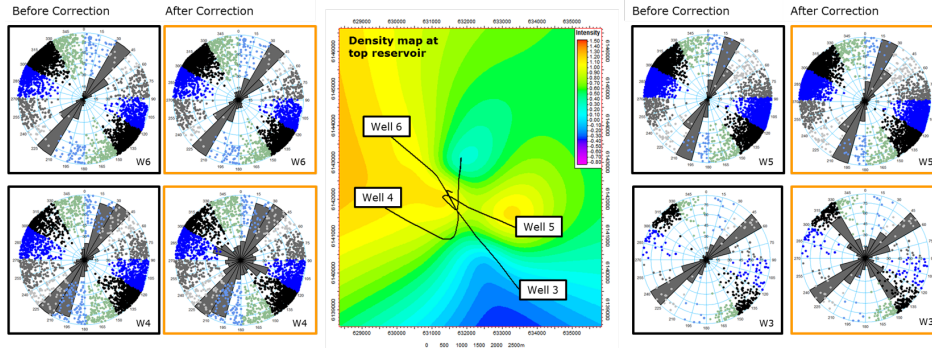


Figure 10: Uncorrected and Terzaghi-corrected strike-rose diagrams from NW-SE oriented wells. Note that the fracture pole data, shown as dots on the stereonets, is uncorrected in both instances.

The uncorrected fracture orientations from the two wells oriented approximately north-south also show a majority of the fractures striking perpendicular to the wellbore (Figure 11). In these wells, however, the relative importance of the fracture set striking perpendicular to the wellbores is significantly reduced after correcting for orientation, and the dominant fracture trend is revealed to strike parallel to the wellbores.

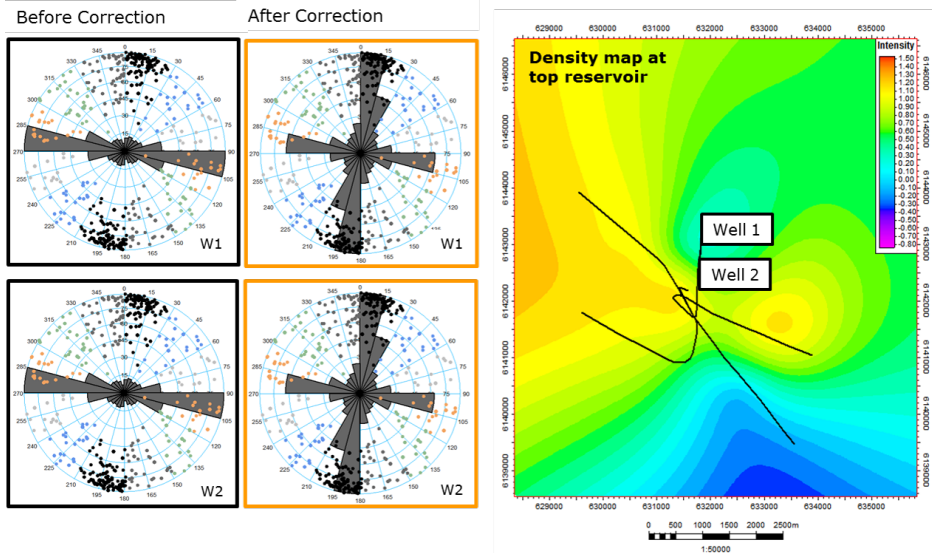


Figure 11: Uncorrected and Terzaghi-corrected strike-rose diagrams from N-S oriented wells. Note that the fracture point data, shown in the stereonets, is uncorrected in both instances.

In the Terzaghi-corrected fracture intensity logs from the seven wellbores, fractures occur as apparent swarms and as isolated features (Figure 12). Relatively high and constant fracture densities are observed in wells 4, 5 and 6. Lower fracture densities and apparent horizontal fracture swarms are observed in wells 1, 2 and 3. The highest fracture density is found in well 7 (vertical) and the lowest fracture density occurs in well 3 (horizontal).

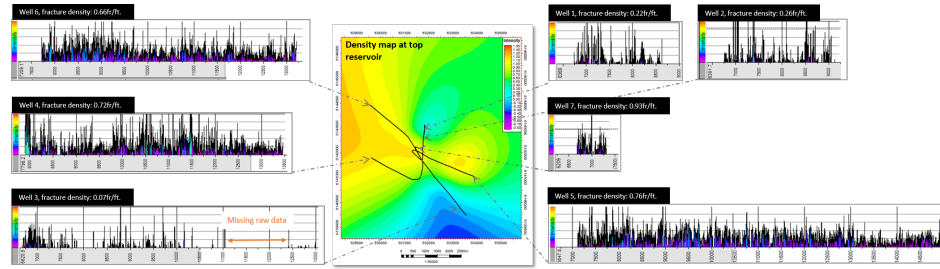


Figure 12: Terzaghi-corrected fracture intensity logs of wells 1-7.

The potential fracture swarm occurrence in the field was further investigated geostatistically. Results were relatively consistent between all investigated wells. Generally, smaller fracture spacings follow a close-to Power law distribution and larger spacings follow a close-to random distribution (Figure 13).

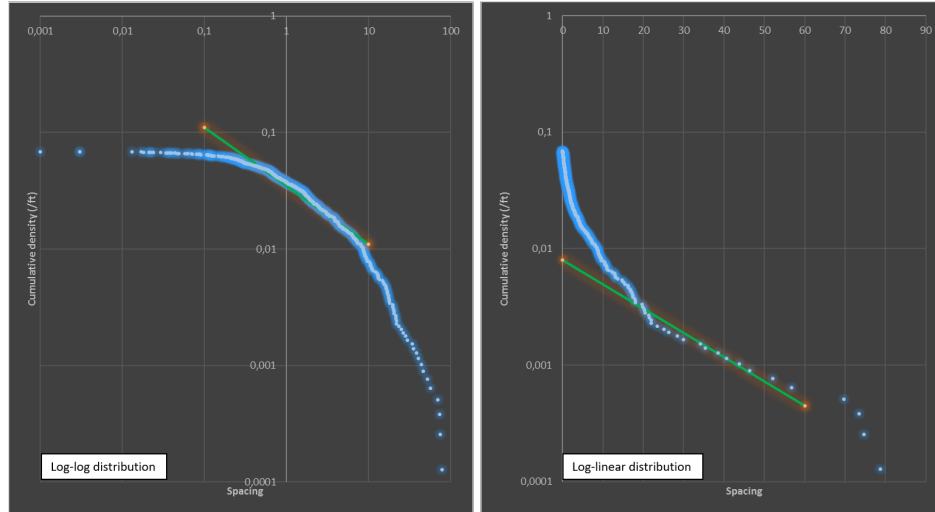


Figure 13: Example of typical spacings distributions of fracture point data in the Kraka Field from well 2.

The value of R in each well is summarized in Table 2. In case of a Power law distribution, the standard deviation should be smaller than the mean, so $R > 1$. In a perfectly random distribution, the standard deviation equals the mean, so $R=1$.

Well	Standard deviation	Mean	R
Well 1	8.3	4.2	2.0
Well 2	9.2	4.4	2.0
Well 3	21.4	7.2	3.0
Well 4	2.7	1.4	1.9
Well 5	2.2	1.2	1.9
Well 6	1.7	1.1	1.5
Well 7	4.5	2.9	1.5

Table 2: Standard deviations and means of Kraka fracture point data.

As the $R > 1$ in all wells, some data clustering occurs in all Kraka wells. This indicates that there is a tendency for fracture swarm occurrence in the field, however R is still quite low, suggesting a signifi-

cant random component in the distribution of fractures in wells 1, 2, 4, 5, 6 and 7. The largest indication of swarming occurs in well 3, which is the well with the lowest fracture density, i.e. the highest mean spacing.

The fracture distribution and the ratio in vertical well 7 is in good correspondence with the horizontal fracture pattern established in the remainder of the BHI-surveyed wells. This indicates a low degree of anisotropy in the Kraka fracture pattern. However, this statements needs further verification through studies of other vertical wellbores.

4.2 Fracture Sets

Collectively, 0.24% of the BHI-fractures are shallow dipping ($<30^\circ$), 24.62% of the fractures have intermediate dip values ($30\text{--}70^\circ$) and 75.14% are steep ($70\text{--}90^\circ$).

Figure 14 shows stereonets and corrected rose diagrams for each stratigraphic unit in each well. Data from the Danian Ekofisk formation is highlighted in green, and data from the Maastrichtian Tor formation is highlighted in red.

We have identified two main fracture trends in the Danian Ekofisk section. The first is a dominant NE/NNE trending regional fracture set, which strikes parallel or near-parallel to the maximum horizontal stress in the area. This main fracture trend is present in the Ekofisk intervals of all horizontal/deviated wellbores and has been confirmed by core data (from wells 1 and 2). Due to data constraints, the vertical fracture distribution of the Kraka Field was primarily studied in well 7. Although the data foundation is insufficient, results from this well indicate that the dominant NE/NNE trend of the Ekofisk formation is vertically continuous.

The secondary fracture set consists of fractures striking parallel and perpendicular to the contours of the Kraka Dome. The orientation of these fractures varies between wells, depending on their location on the dome. This fracture set is thought to have formed during salt movements, and it is expected to follow the strain evolution of the Kraka chalk. Because of the positions of wells 5 and 6, the two fracture sets in cannot be distinguished on the basis of orientation in these wells (the dome contours are parallel to the NE/NNE regional trend).

The NNE/NE trending regional fracture set continues into the Tor Formation of wells 2, 6 and 7. However there is much more scatter in the Tor orientation data than in the Ekofisk data. The scattering may be due to varying local stresses during salt movements, however there is insufficient data from the Tor Formation to determine the fracture pattern with confidence.

5 Seismic-scale Fault Trends

There is a good correlation between fracture orientations on BHIs and the orientation of seismic scale lineations, as shown in Figure 15. The RGB ant-tracked structural model contains 25 lineations. The majority (16) of these lineations strike NNE/NE. The main NE/NNE fracture trend can thus be correlated from well scale to ant-tracked scale. Of the 32 large-scale faults interpreted on amplitude seismic, 18 are oriented in a NE direction, while only 3 faults strike NNE. This indicates that the NNE trend is representative for smaller-scale lineations, below the resolution of amplitude seismic and for well-scale fractures.

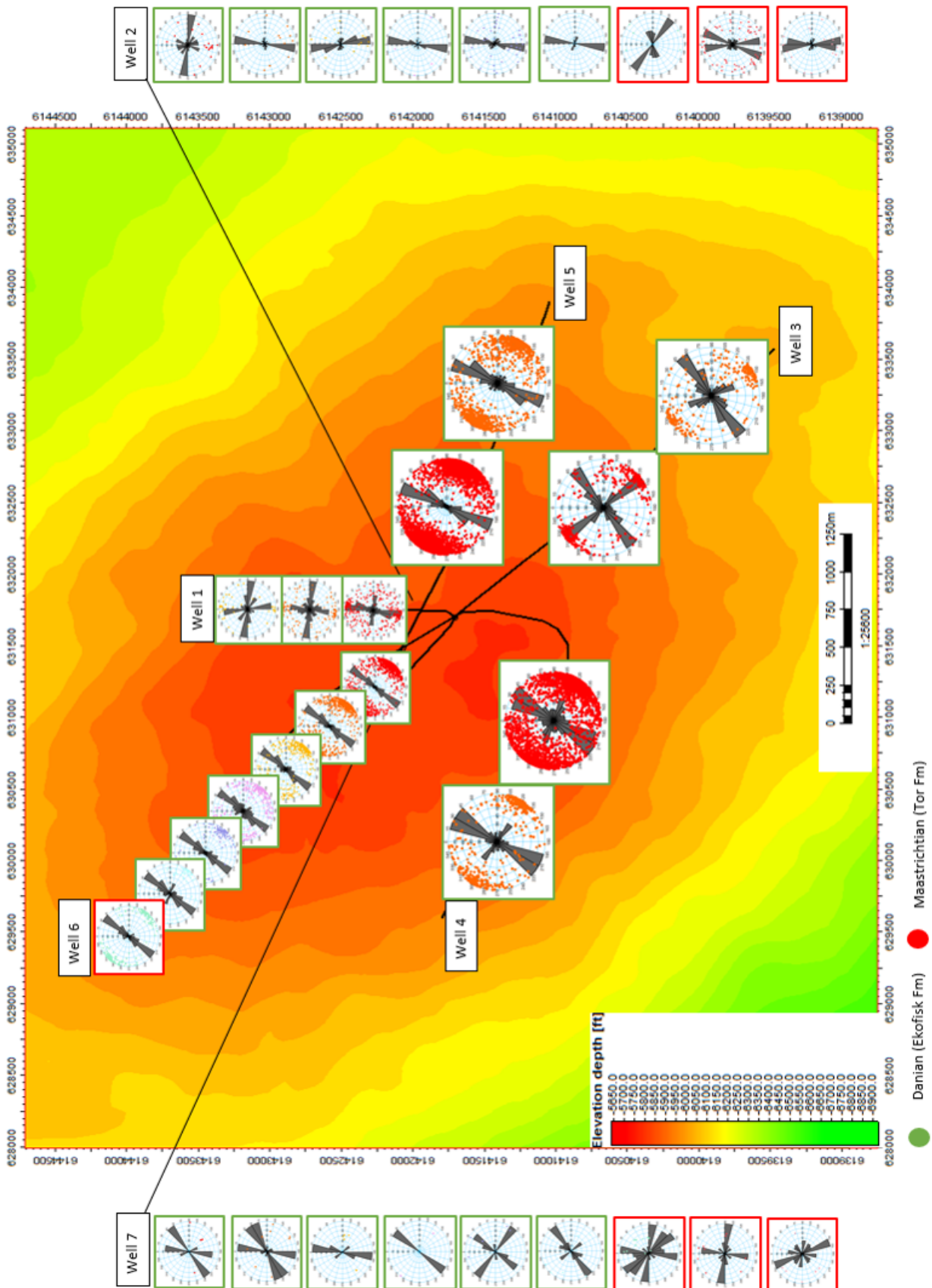


Figure 14: Fracture point data and corrected rose diagrams in wells 1-7, plotted after unit on the top reservoir depth map.

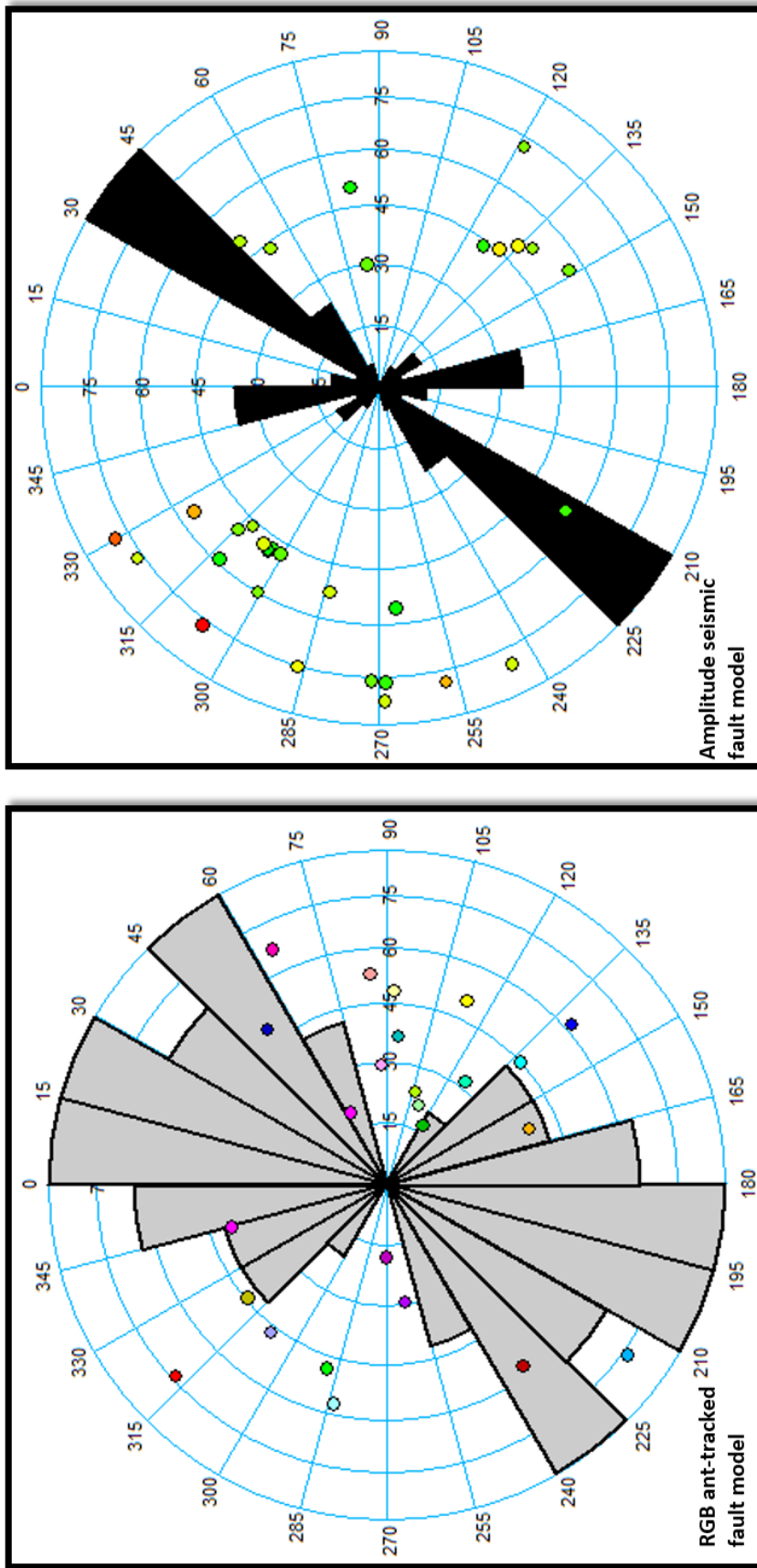


Figure 15: Rosediagrams of structural lineations interpreted on the RGB ant-tracked volume (left) and the amplitude volume (right).

6 Conclusions

We have developed an integrated workflow for correlation of structural features at different scales in chalk reservoirs. Results from the Kraka Field, which was chosen as a test-case, indicate that:

1. A large portion of extensional and chert-associated fractures identified in core are distinguishable in borehole images. Styrolites, stylolite-associated fractures, fractures located in bioturbated zones and well-parallel fractures are however difficult to differentiate in the BHIs.
2. Borehole images are imperative in distinguishing cemented from open fractures, as as cemented fractures may be opened during the coring process. BHIs thus increase our ability to constrain fluid flow along the fracture network.
3. Extensional and chert-associated fractures are commonly represented by partial sinusoids in BHIs, suggesting they are either short or only partially open or cemented.
4. Manual dip-picking was deemed requisite because of:
 - The large portion of fractures represented by partial sinusoids.
 - Relativley poor image quality (compared to to newer BHI data).
 - Internal resistivity variations, which may “confuse” automatic dip-picking tools.
5. For the ant-tracked algorithm, higher vertical resolution can be achieved through RGB image processing, compared to wavelet based extraction of structural features. Both ant-tracked volumes display structural trends that are below the resolution of amplitude seismic.
6. Fractures picked on BHIs correlate to large-scale regional trends and to features picked on ant-tracked seismic data. This strengthens the case of a consistent regional stress field that scales down to local stresses observed at the BHI and core scale. We can therefore extrapolate fractures away from the wellbores and calibrate 3D models (e.g. discrete fracture network models).

The Ekofisk Formation of the Kraka Field is characterized by steep fractures striking NE and NNE, parallel or near-parallel to the maximum horizontal stress in the area. Fractures in Kraka occur as swarms and as isolated features. Moderate fracture clustering occurs in the majority of horizontal wells, as well as in the vertical well. The greatest tendency for fracture swarm occurrence is observed in the horizontal well with the lowest associated fracture density.

The main fracture trend, established from borehole images and core, is present in the Ekofisk sections of all horizontal/deviated wellbores and has been confirmed by core data. Results from the vertical well 7 indicate that the dominant NE/NNE trend of the Ekofisk Formation is vertically continuous.

A secondary fracture set of fractures striking parallel and perpendicular to the contours of the Kraka Dome was identified. The orientation of these fractures varies between wells, depending on their location on the dome. This fracture set likely developed during salt movements and is expected to follow the strain evolution of the Kraka chalk.

The main NNE/NE fracture trend can be correlated from well scale to ant-tracked scale. Faults mapped on amplitude seismics can also be identified in the ant-tracked cube. In the amplitude model, faults mainly trend NE, indicating that the NNE trend is representative for smaller-scale lineations (well scale to ant-tracked scale).

This integrated study proves invaluable in testing assumptions in building fracture models and the subsequent upscaling process and will be useful for validating a geomechanically based DFN for the Kraka Field.

7 Acknowledgements

The research leading to these results has received funding from the Danish Hydrocarbon Research and Technology Centre under the Advanced Water Flooding programme. We thank DUC for providing data access. We would also like to extend our thanks to Schlumberger for providing licenses for Petrel, eXchroma and Techlog.

Fernø, M. A., 2012, Enhanced Oil Recovery in Fractured Reservoirs, In: Romero-Zerón, L. (ed.), Introduction to Enhanced Oil Recovery (EOR) Processes and Bioremediation of Oil-Contaminated Sites, p.89-110

Gillespie, P. A., Howard, C. B., Walsh, J.J & Watterson, J., 1993, Measurement and characterisation of spatial distributions of fractures. *Tectonophysics*, v. 226, p.113-141

Gillespie, P. A., Walsh, J. J., Watterson, J., Bonson, C. G. & Manzocchi, T., 2001, Scaling relationships of joints and vein arrays from the Burren, CO. Clare, Ireland. *Journal of Structural Geology*, v. 23, p.183-201

Jørgensen, L. N. & Andersen, P. M., 1991, Integrated Study of the Kraka Field: paper presented at the 1991 Offshore Europe Conference, Aberdeen, Scotland (SPE 23082)

Klinkby, L., Kristensen, L., Nielsen, E. B., Zinck-Jørgensen, K. & Stemmerik, L., 2005, Mapping and characterization of thin chalk reservoirs using data integration: the Kraka Field, Danish North Sea, *Petroleum Geoscience*, Vol. 11, p. 113–124

Koestler, A. G. & Reksten, K., Insight into the 3D Fracture Network of an Exposed Analogue of Fractured Chalk Reservoirs. The Lägerdorf Case: paper presented at the 1992 Fourth North Sea Chalk Symposium, Deauville, France.

Laake, A., 2015, Structural interpretation in color - A new RGB processing application for seismic data: *Interpretation*, Vol. 3, Issue 1, p. SC1–SC8

Møller, J. & Rasmussen E. S, 2003, Middle Jurassic – Early Cretaceous rifting of the Danish Central Graben, In: Inseon, J. R. Surlyk, F. (eds.), Geological Survey of Denmark and Greenland Bulletin 1, p.247–264 Olson, J., E., Predicting fracture swarms - the influence of subcritical crack growth and the crack-tip process zone on joint spacing in rock. *Geological Society, London, Special Publications* 2004, v. 231, p. 73-88

Pedersen, S. I., Randen, T., Sonneland, L. & Steen, O., 2005, Automatic fault extraction using artificial ants, In: Iske A. & Randen T. (eds.), *Mathematical Methods and Modelling in Hydrocarbon Exploration and Production. Mathematics in Industry*, Vol 7., p.512–515

Rank-Friend, M. & Elders, C. F, 2004, The evolution and growth of Central Graben salt structures, Salt Dome Province, Danish North Sea, In: Davies, R. J, Cartwright, J. A, Stewart, S. A., Lappin, M. Underhill, J. R. (eds.) *3D Seismic Technology: Application to the Exploration of Sedimentary Basins*. Geological Society, London, Memoirs, Vol. 29, p. 149-163

Rasmussen, E. S., Vejbæk, O. V., Bidstrup, S. & Dybkjær, K., 2005, Late Cenozoic depositional history of the Danish North Sea Basin: implications for the petroleum systems in the Kraka, Halfdan, Siri and Nini fields, In: Dorè, A. G. Vining, B. A (eds.), *Petroleum Geology: North-West Europe and Global Perspectives— Proceedings of the 6th Petroleum Geology Conference*, p.1347–1358

Schlumberger, 2006, Fault Resolution Improved for Norsk Hydro's Varg Field. Case study: Variance Cube software enhances imaging and reduces processing time, [online], accessed November 20th 2017, http://www.slb.com//media/Files/software/case_studies/varcube.cs.ashx